The Role of Melt-pool Behavior in Free-jet Melt-spinning

Personnel: R.E. Napolitano (PI) and H. Meco (Postdoc)

Scope:

The influence of melt-pool behavior on the competition between nucleation of crystalline solidification products and glass formation is examined for an Fe-Si-B alloy. High-speed imaging of the melt-pool, analysis of ribbon microstructure, and measurement of ribbon geometry and surface character all indicate upper and lower limits for melt-spinning rates for which fully amorphous ribbons can be achieved. Comparison of the relevant time scales reveals that surface-controlled melt-pool oscillation may be the dominant factor governing the onset of unsteady thermal conditions accompanied by varying amounts of crystalline nucleation observed near the lower limit. At high rates, the influence of these oscillations is minimal due to very short melt-pool residence times. However, microstructural evidence suggests that the entrapment of gas pockets at the wheel-metal interface may play a critical role in establishing the upper rate limit. An observed transition in wheel-side surface character with increasing melt-spinning rate supports this contention. The upper velocity bound for the production of uniform amorphous ribbons during free-jet melt-spinning is predicted by coupling a mass-balance condition for the melt-pool with a simple boundary-layer model for momentum transfer. The relationships between melt-pool length, ribbon thickness and wheel speed were thus investigated, and a criterion was developed for the onset of unsteady melt-pool behavior, which has previously been associated with increased surface roughness, porosity, and the formation of crystalline phases at high wheel speeds.

Research Highlights

In this processing science study we investigated the role of melt-pool behavior on microstructure formation during free-jet melt-spinning, where a stream of molten metal is poured or injected under pressure so that it strikes a rotating chill wheel. Generally, bulk cooling rates increase with increasing wheel rotation speed and a minimum wheel speed can be identified below which crystalline phases are observed. However, for an $Fe_{75}Si_{10}B_{15}$ alloy, we have observed that a specific range of intermediate spinning rates exists within which the melt pool remains steady, and uniform amorphous ribbons are produced. At higher or lower wheel speeds, crystalline phases are observed. The presence of this "window", particularly its upper bound, cannot be explained by the bulk cooling rate dependence on wheel speed. Rather, experimental evidence suggests that local thermal transients arising from unsteady melt-pool behavior and the entrapment of gas at the melt-wheel interface each play a critical role in establishing these observed regimes of nucleation behavior. Even when bulk cooling conditions are conducive to glass formation, local conditions may be substantially altered by melt-pool phenomena such that ribbons exhibit high surface roughness, porosity, and crystalline phases, which typically nucleate and grow near entrapped gas pockets, as shown in Fig.1. Thus, the reliable production of amorphous ribbons through the free-jet melt-spinning process requires that the process be conducted under conditions giving rise to a steady melt pool where the formation and entrapment of gas pockets does not occur.

We examined these limits for stable melt-spinning and amorphous ribbon production and we have developed an analytical criterion for the lower limit, where the appearance of crystalline phases is indicated by the condition where the melt-pool residence time becomes comparable to the low-mode natural oscillation frequencies of the melt-pool (Fig.2). These depend

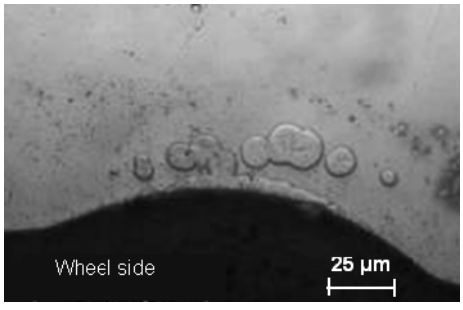

Fig. 1 Nucleation of crystalline nodules on entrapped gas pockets on the wheel-side surface of a melt spun ribbon.

primarily on the fluid mass contained within the melt-pool and the liquid-vapor surface tension. Thus, it is the increase in melt-pool mass that accompanies decreasing wheel speed that ultimately causes the change in melt-pool behavior associated with the observation of crystalline phases below the observed lower limit. For the upper limit, we have developed an analytical criterion for the onset of gas entrapment and non-uniform cooling by considering the constraints of mass balance and momentum transfer within the melt pool. Based on a simple fluid flow analysis, the unsteady behavior and gas entrapment observed can be attributed to insufficient feeding volume, for the given incoming stream diameter. Experimentally, we find that our prediction of the high velocity limit does indeed correspond to a break-down in stable melt-pool behavior, characterized by increased wheel-side surface roughness, porosity, and the nucleation of crystalline phases near entrapped gas pockets. Accordingly, our model suggests that this upper bound can be increased (extending the "window" of steady melt-pool behavior to higher speeds) by increasing the injection velocity or decreasing the injection stream diameter.

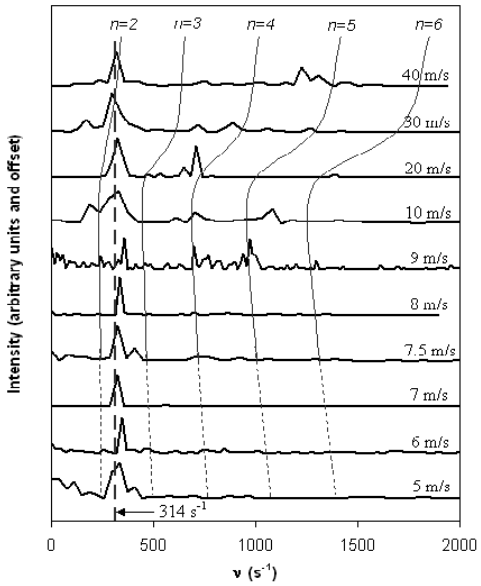

Fig. 2 Fourier transform of ribbon width showing a characteristic frequency of ~ 314 s^{-1} for all wheel speeds, falling between predicted *n*=2 and *n*=3 oscillation modes.

Impact:

As in all solidification processes, the resulting microstructure is governed largely by the competition between various nucleation and growth mechanisms. In many casting processes, the conditions which give rise to nucleation may be selectively promoted or suppressed, and the microstructure can be controlled accordingly. This is far from the case for the melt-spinning process, where the thermal conditions are neither easily controlled nor well understood. Various modeling approaches and analytical treatments have made some progress toward the general prediction of thermal conditions within the melt-pool. Since melt-spinning is often implemented to achieve rates sufficiently high to avoid nucleation altogether, resulting in an amorphous or glassy ribbon, nucleation control is of primary importance. However, nucleation kinetics are generally very sensitive to local temperature, with volumetric nucleation rates generally varying as $\exp(-1/T\Delta T^2)$ and microstructural control remaining problematic. To this end, we offer several observations regarding nucleation and growth during the melt-spinning of Fe-Si-B alloys with the intent that these may provide some insight into the important effects of fluid flow and gas entrapment as they become significant factors in the melt-pool within different regimes of quench-wheel velocity.

Future Work:

As a result of this work, we have gained fundamental insights on the role of the melt pool during microstructure formation in melt-spinning. This understanding will facilitate current and future investigations of solidification at high undercooling and of glass formation. Coupled with a new generation melt-spinning facility and emerging high speed imaging capabilities, this work will lead to an ability to predict and control the various phenomena that may occur under these far-from-equilibrium conditions.

Interactions:

This work will contribute to various efforts within the Program, including the effort entitled, "Solidification in eutectic systems driven far from equilibrium."

Phase Diagram Determination for Binary R-Ni (R=Nd, Pr) Systems

Personnel: T.A. Lograsso (PI), R.W. McCallum (PI), and M. Huang (Postdoc)

Scope:

High quality single-phase single crystal/polycrystal of the $R_{(n+1)(n+2)}Ni_{n(n-1)+2}Si_{n(n+1)}$ series of compounds are needed for the research within the Magnetism Focus Area. However, due to the lack of detailed phase diagram information, considerable difficulties have been encountered in the preparation of these compounds. Therefore, thermodynamic descriptions for the R-Ni-Si (R=Ce, La Nd, Pr) systems are desired by using both experiment and thermodynamic modeling to facilitate the crystal growth. To accomplish this goal, a processing science investigation commenced to determine phase equilibria in the limiting binary systems by employing both experimental and computational methods.

Research Highlights:

The Ni-Pr and Nd-Ni systems were investigated via experiments and thermodynamic modeling. Alloys across the entire composition range in both the Ni-Pr and Nd-Ni systems were prepared by arc melting followed by homogenization, and then subjected to investigation using thermal analysis and scanning electron microscopy. The existence of the reported stoichiometric compounds in both systems was confirmed. Although the temperature difference between our results and those reported for the Nd-Ni system is not large (20-50 °C), significant difference (30-100 °C higher) was found for congruent melting of the compounds and the invariant reactions in the Ni-Pr system, especially on the Pr-rich side. Except for the peritectic reaction, liquid + $Nd_7Ni_3 \leftrightarrow Nd_3Ni$, and the polymorphous phase transformation of Nd_2Ni_7 found in the Nd-Ni system, all the other invariant reactions in both binaries are confirmed to be the same type, but with significantly different temperatures from those reported.

In the modeling part, the available phase equilibrium and thermodynamic data in the Ni-Pr and Nd-Ni systems were analyzed by using thermodynamic models for the Gibbs energies of individual phases. An optimal set of thermodynamic parameters for Ni-Pr and Nd-Ni binaries were obtained (see figures).

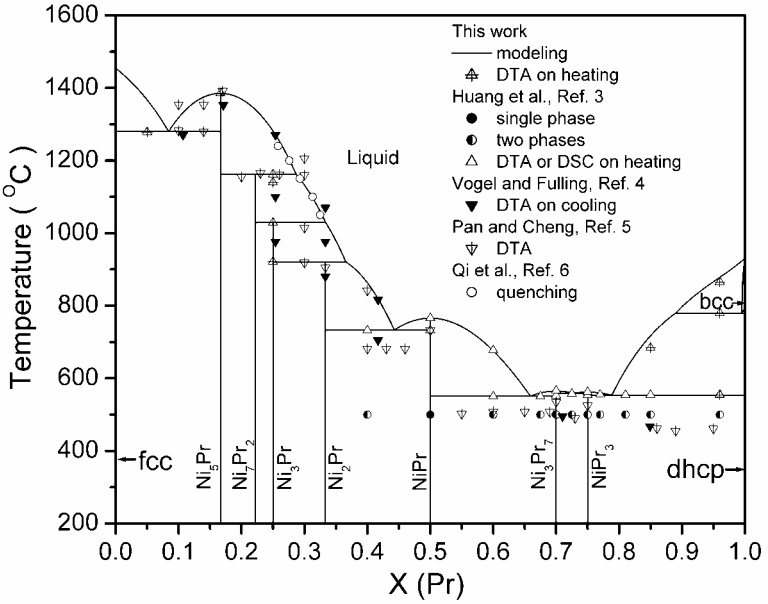

Fig. 1 The calculated Ni-Pr binary together with experimental data

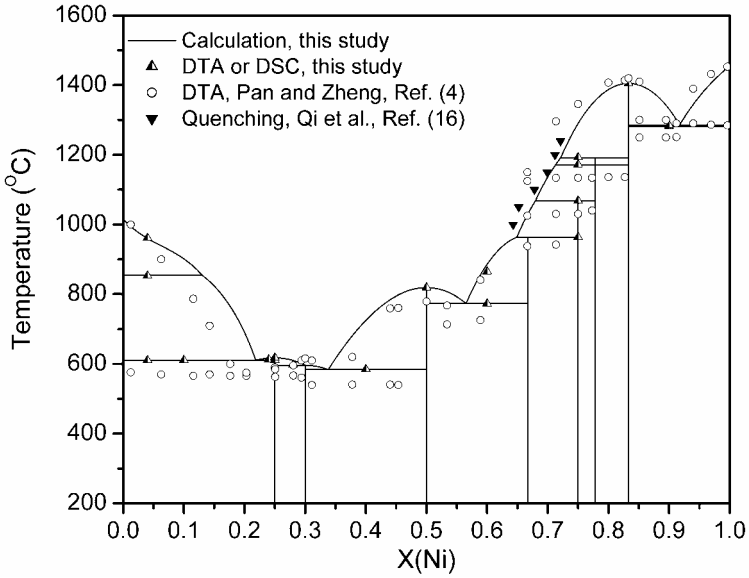

Fig. 2 The calculated Nd-Ni binary together with experimental data

Significance:

Significant differences (30-100 °C higher) have been found for congruent melting and invariant reaction temperatures in the Ni-Pr system compared to what has been published. In addition, a different reaction type for the compounds Nd_7Ni_3 and Nd_2Ni_7 were found in the present study compared with literature data. Improved thermodynamic descriptions were obtained for the Nd-Ni and Ni-Pr binaries based on reported thermodynamic data and the current experimental results, which will help to obtain more accurate phase diagrams for the R-Ni-Si (R=Ce, La, Nd, Pr) ternary systems. The ability to calculate and predict the ternary phase diagrams for these systems has led directly to significant improvements in the synthesis of single crystalline compounds of interest in the Pr-Ni-Si. (See Magnetism Focus area highlight – "Thermodynamic Modeling and Flux Growth of Single Crystals of the R-Ni-Si Systems")

Future Accomplishments:

Our goal is to obtain reliable phase diagrams for the R-Ni-Si (R=Ce, La, Nd, Pr) systems. More detailed phase diagram studies will be conducted to facilitate the preparation of the compound series $R_{(n+1)(n+2)}Ni_{n(n-1)+2}Si_{n(n+1)}$, in which R is Ce, La, Nd and Pr. Specifically, investigations will be carried out on the Ce-Ni, Ce-Si, La-Ni, Nd-Si, and Pr-Si binary systems via experimental and thermodynamic modeling. Alloys in the five binary systems will be prepared by arc melting and homogenized in the furnace and subjected to investigation using thermal analysis and scanning electron microscopy. Thermodynamic models for Ce-Ni, Ce-Si, Nd-Ni, Nd-Si and Pr-Si binary systems will be developed and finally the liquidus surface for the R-Ni-Si systems will calculated.

Interactions:

This work is in collaboration with the other programs in the Magnetism Focus area.

Time-Resolved Neutron Diffraction of Actively-Reinforced Composites During Consolidation Processing

Personnel: I.E. Anderson (PI), S.B. Biner (Co-PI), Collaborators: F. Tang (ORNL), and D. Brown (LANL)

Scope:

An exploration is being conducted of the materials and processing parametrs needed to exploit the benefits of composite material strengthening by active reinforcement phases that undergo transformation during composite processing. These novel materials were discovered as a result of tensile testing of Al/Al-Cu-Fe composites that revealed impressive gains in the yield and ultimate tensile strength, beyond what could be attributed to improved, interparticle bonding. By X-ray diffraction, the initially quasicrystalline (ψ-phase) $Al_{65}Cu_{23}Fe_{12}$ (reinforcement) particles in Al/Al-Cu-Fe composites (from 15-30 vol.% reinforcement) were found to have reacted with the Al matrix at some time during consolidation and were transformed into a less dense crystalline Al_7Cu_2Fe (ω) phase. Because of the density difference of the ψ (4.7 g/cm^3) and ω (4.08 g/cm^3) phases, the volume of the reinforcement particles expanded about 12%, assuming complete ψ to ω phase transformation. This positive transformation strain, acting on the matrix phase within the confinement of the hot pressing or forging die, was the likely source of large compressive residual stresses that were observed by neutron diffraction in the Al matrix after consolidation of a series of composite samples. Tensile testing of Al/Al-Cu-Fe composite specimens, after high temperature stress relaxation, resulted in a significantly reduced strength, confirming the major influence of compressive residual stress on strengthening. The purpose of this processing study is to better assess via time-resolved neutron diffraction the phase transformation behavior in this system and how compressive stress formation and relaxation kinetics may be controlled.

Research Highlights:

The in-situ neutron diffraction measurements were performed during vacuum hot pressing (VHP) of Al/Al-Cu-Fe composites on the SMARTS diffractometer at the Lujan Center for Neutron Scattering at Los Alamos National Lab. The SMARTS load-frame/furnace was fitted with a V-12Nb (wt.%) VHP die set that we designed and built to provide consolidation confinement without neutron beam interactions, allowing in-situ time-resolved neutron diffraction measurements of each powder compact during VHP. Thus, the phase transformation and phase stress evolution in an Al/Al-Cu-Fe composite was successfully measured at intervals during a typical consolidation cycle (see Fig.1), including events labeled (on x-axis) for: a) room temperature (RT); b) max. temp., 600ºC; c) load applied, 290 MPa; d) load released; e) cooling started; and f) RT. Fractional changes in the interplanar spacing from all of the diffracting phases detected in the neutron measurement volume are summarized in Fig. 1. Analysis of Al and ω-phase peak displacement at 600ºC indicated that a simultaneous increase of compressive strain was found in both phases of the composite during compaction. After release of the compaction pressure, 600ºC was maintained briefly to investigate annealing effects, confirming a partial stress relaxation for both Al- and ω-phases, before slow cooling to ambient temperature. Neutron diffraction data (see Fig. 2) that were collected at the event points labeled on each scan show: i) Al (fcc) lattice expansion on heating from RT to 600ºC (a to b), with quasicrystalline reflections retained on heating, before applied pressure; ii) quasicrystalline peaks disappear, essentially, and ω-phase peaks appear within 15 minutes (the measurement interval) of applied pressure (b to c); and iii) Al (fcc) and ω-phase lattice peaks contract on cooling to RT (c to f). The rapid ψ to ω phase transformation kinetics apparently were promoted by the high pressing temperature and full contact of deformed particle surfaces, and accomplished by diffusion of Al from the high purity Al matrix (crossing prior particle boundaries) into the ψ-phase particles. It

should be noted that previous Auger results indicated no significant reverse diffusion of Cu or Fe to the Al matrix. The final residual stress of the Al matrix, after extraction of the consolidated composite sample, was still compressive, in agreement with previous measurements on the same composite, but significantly reduced, certainly by the unconfined annealing at 600ºC (d to e).

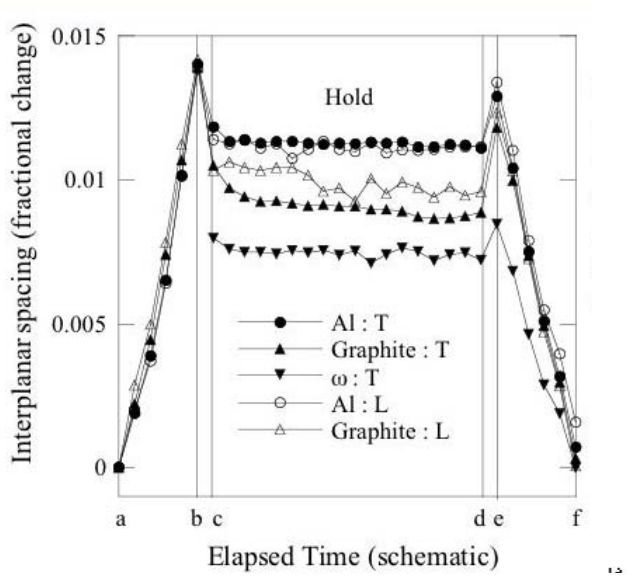

Fig. 1

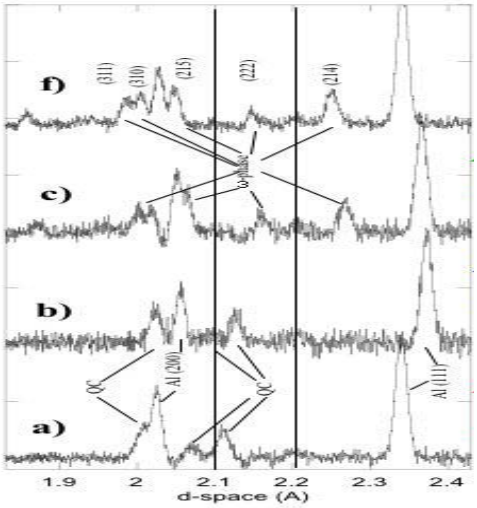

Fig. 2

Impact:

A high residual compressive stress should have a beneficial effect on fatigue life, especially high cycle fatigue, where it can be considered to adjust upward the stress plateau for "infinite lifetime." The same desirable state of residual compressive stress may be possible to induce by a selected processing route in several other types of matrix metals with a variety of other reinforcement phases. This could present a new paradigm in the selection of material systems and processing methods for composite materials.

Future Work:

Pending funding, experimental efforts would continue in the time-resolved neutron diffraction of actively-reinforced composites during consolidation processing to separate effects of densification and diffusion-controlled phase transformation of reinforcement phase. These new results would add knowledge about phase and stress evolution in this important new type of actively-reinforced composite material that can permit modeling of the dynamic stress state in this complex type of microstructure. Additional support is thus needed for design of alternative actively-reinforced composite systems to test the generality of the compressive residual stress effects and to permit tailoring of the properties of these novel material systems.

Interactions:

This effort has benefited from studies in the Science of Amorphous and Aperiodic Materials Focus Area. Interactions with D.J. Sordelet and M.J. Kramer comprise ongoing efforts to provide additional understanding of quasicrystal transformation pathways and interdiffusion effects.